DOI 10.1007/s10517-020-04719-7

METHODS

Real-Time Recording and Processing of Spike Electrical Activity of the Small Intestine in Experiments on Rats

A. V. Zherebtsov and N. S. Tropskaya

Translated from *Byulleten' Eksperimental'noi Biologii i Meditsiny*, Vol. 168, No. 9, pp. 383-386, September, 2019
Original article submitted April 8, 2019

Real-time recording technique and mathematical processing of the spike electrical activity in the small intestine were developed for chronic experiments on rats. Open-source software was employed to digitize electromyograms and to process them in a real-time mode with a fourth-order nonlinear differential energy operator. This method improved identification of spike electrical activity in the small intestine in experiments.

Key Words: *spike electrical activity; small intestine; electromyogram processing; nonlinear differential energy operator*

Electrical activity of the small intestine manifests itself by two dominant components: slow waves (SW) and spike potentials (SP) [10]. SW are not directly responsible for intestinal contractile activity, but play the coordinating and synchronizing roles in contractions. In contrast, SP directly correlate with contractile activity [10]. SP can be presented by single voltage impulses or bursts appearing at the crest of SW. The SP bursts can appear at different periodicity thereby forming various intestinal rhythms such as minute rhythm or rhythmic phase III of the migrating motor complex [2].

There are effective algorithms to precisely analyze the frequency and amplitude of SW and to identify the crests of each SW [1,3]. In contrast, automatic analysis of SP is more complicated because of the artifacts (including those originating from electrical activity of the heart), which frequently have SP-like shape. In addition, the non-infrequent abrupt falling edges of SW [12] can distort filtering in the frequency band of SP.

N. V. Sklifosovsky Research Institute of Emergency Medicine, Moscow Department of Health Care, Moscow, Russia. ***Address for correspondence:*** aleksey1235@mail.ru. A. V. Zherebtsov

To develop effective algorithms for analysis of SP in neurograms, electromyograms (EMG), and *QRS* components of ECG, the researches advanced a nonlinear energy operator (NEO) or Teager—Kaiser energy operator [4,6,8]. Specifically, there are NEO-based threshold algorithms to identify SP in the small intestine. One of such algorithms identifies SP recorded via a multielectrode array located on intestinal seromuscular layer. This algorithm is based on NEO coupled with the threshold identification of SP. However, the choice of the threshold for SP identification needs rather complicated procedures with numerous calculations over the large EMG segments. At present, it is problematic to realize such algorithms to identify SP with sufficient accuracy in real-time mode. Importantly, one of the troubles in recording with a multielectrode arrays is their use only in acute experiments on narcotized animals. The available literature does not report the methods to record and identify SP in real-time mode during chronic experiments on non-narcotized animals.

This work was aimed at developing a method of recording and identification of electrical spike activity in the small intestine during chronic experiments on non-narcotized rats.

Preliminary, 3 needle monopolar electrodes were implanted into seromuscular layer of the small intestine at the interelectrode distance of 5 cm. The reference electrode was fixed to anterior abdominal wall. The electrode wires were passed out of the body through the tail with the help of a thin conductor. During experiments, the rats were fixed in a metal cage with a collar that was attached to the tail with a needle. The cage was electrically connected to the ground input of a 48-channel NVX-52 encephalograph. Four channels were connected to 3 recording and 1 reference electrodes.

OpenViBE open-source software capable to drive NVX-52 encephalograph was employed to record, process, and display signals [9]. This software consists of individual modules, which we supplemented with original DEAO module written in Python to realize the parallel processing of the recorded signals. The modular structure of employed software (Fig. 1) made it possible to perform simultaneous experiments with several rats according to the number of implanted electrodes and the number of recording channels in an amplifier. Here, Acquisition Client Module coupled to encephalograph yielded 4 EMG per rat, one of which was used as Reference Channel. To eliminate a low-frequency trend and high-frequency interference artifacts, initial (raw) EMGs were processed with a band-pass filter (0.1-35.0 Hz) realized in a Temporal Filter module (Fig. 1). Then the signals were merged into combined data flow by Signal Merger module (Fig. 1). Signal Display, Signal Display HF, and Spike Signal Display modules sequentially display (one under another) the original and processed signals.

Generally [7], a k-order differential energy operator for discrete signal x is defined as:

$$Y_k(x[n])=x[n]x[n+k\text{-}2]\text{-}x[n\text{-}1]x[n+k\text{-}1], \quad k=0,1,2,3\ldots \qquad \textbf{(1)}$$

NEO is a special case of differential energy operator for k=2:

$$Y_2(x[n])=x[n]x[n]\text{-}x[n\text{-}1]x[n+1]. \qquad \textbf{(2)}$$

NEO simultaneously characterizes instantaneous amplitude and frequency of the processed signal. Thus, it can assume different values for the signal segments with equal amplitudes but different frequency composition. Comparison of SP identification in a realistic simulation of extracellular signal performed by NEO and 4-order differential energy operator with the same method of threshold selection showed that the latter yielded more reliable results despite comparable computational complexities [11]. The 4-order differential energy operator is known as discrete energy acceleration operator (DEAO):

$$Y_4(x[n])=x[n]x[n+2]\text{-}x[n\text{-}1]x[n+3]. \qquad \textbf{(3)}$$

Here, we employed DEAO to extract SP from intestinal EMG. Prior to DEAO, the low-frequency components in raw signal (SW included) were elim-

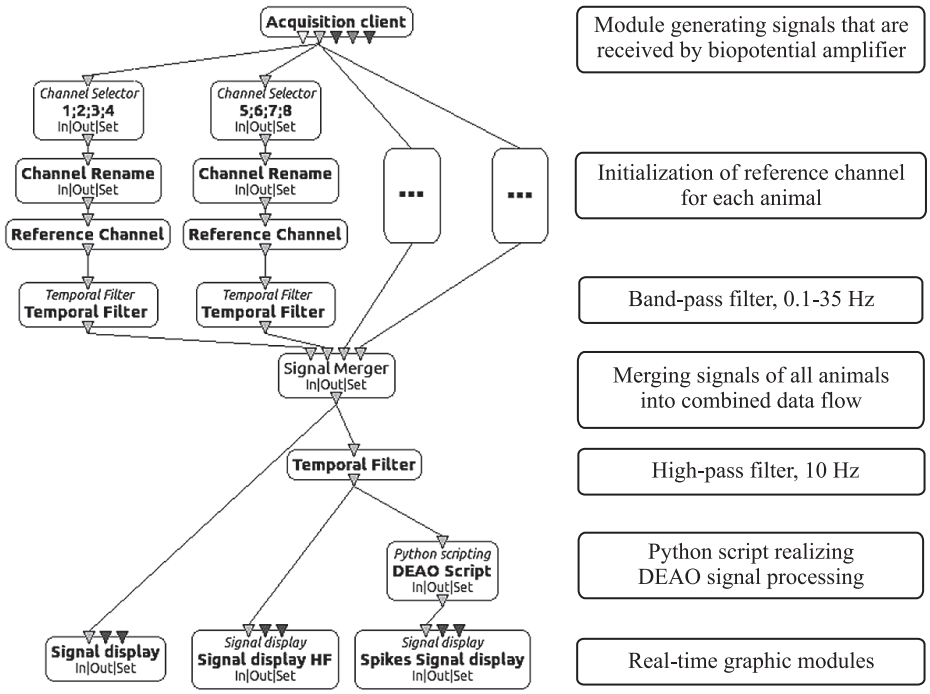

Fig. 1. Modul block diagram realized in OpenViBE software. Ellipsis marks a set of modules, which are similar to adjacent ones. The number of such modules depends on the number of rats in the examined group.

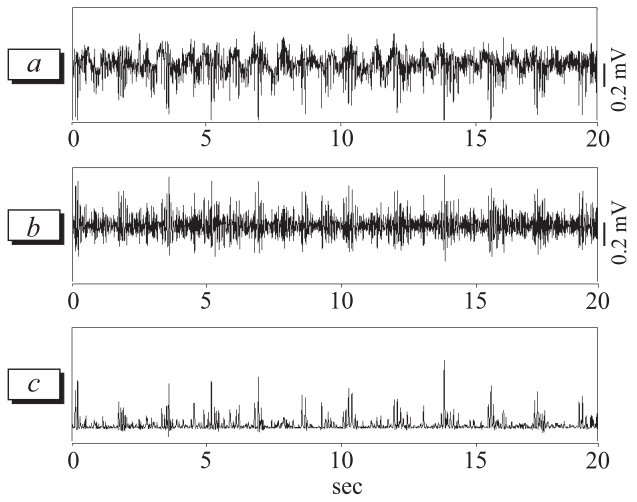

Fig. 2. SP in EMG recorded from small intestine. Initial EMG (*a*) and the same record processed with a 10 Hz high-pass filter (*b*) and then with DEAO algorithm (*c*).

inated by a 4-pole high-pass Butterworth filter with the cutoff frequency of 10 Hz. The resulting high-frequency records with SP were processed with DEAO.

Figure 2 shows a raw EMG with SP and SW, filtered EMG containing only SP, and DEAO-processed EMG with extracted SP. Evidently, the high-amplitude SP bursts in filtered EMG corresponded to those in DEAO-processed traces, but DEAO pronouncedly suppressed the signals between these bursts. Thus, DEAO extracted SP bursts against the background noise and artifacts, whose amplitude-frequency characteristics differed from those of SP.

Figure 3 shows two jejunal EMGs recorded in a rat on day 4 after implantation of the needle electrodes into proximal and distal subdivisions of the jejunum at a distance of 5 and 10 cm, respectively, from the ligament of Treitz. The interelectrode distance was 5 cm. The raw EMGs incorporated both artifacts and analyzed signals including SP and SW (Fig. 3, *a*). The high-pass filtering and DEAO-processing clearly revealed EMG segments, which contained no SP or had small- or high-amplitude SP (Fig. 3, *b*). The length of such segments can be easily measured or visually assessed. Actually, consider an SP-free part of DEAO-processed EMG recorded in proximal subdivision of the jejunum (Fig. 3, *b*, segment 600-656 sec). In contrast to processed EMG, this segment of raw EMG included the artifacts (interference from ECG), where it was impossible to establish the absence of SP. Actually, consider the segment of EMG with high-amplitude SP in both parts of the jejunum. The raw EMGs (Fig. 3, *a*) contain this segment, but it cannot be unequivocally described because of interference from the artifacts. In contrast, it can be easily made in the transformed EMG (Fig. 3, *b*). Actually, the periods of high-amplitude SP were 656-797 sec and 709-850 sec in proximal and distal jejunal subdivisions, respectively. Thus, the durations of high-amplitude SP bursts were identical (141 sec) in both parts of the jejunum, which is far from being evident in raw EMGs. These high-amplitude SP bursts were generated in two neighboring parts of the jejunum with the time difference of 53 sec. Since the interelectrode distance was 5 cm, the wave front of high-amplitude SP bursts propagated along the jejunum with velocity of 0.094 cm/sec (5.66 cm/min).

Thus, a method of real-time EMG processing was developed with open-source software, which essentially improved identification of spike-like electrical activity of the small intestine and jejunum in experimental animals. This method is based on high-pass filtering of EMG followed by it processing with DEAO. The advanced method can assess the parameters of regular electrical spike activity (duration and propagation velocity) corresponding to different peristalsis modes of the small intestine and jejunum.

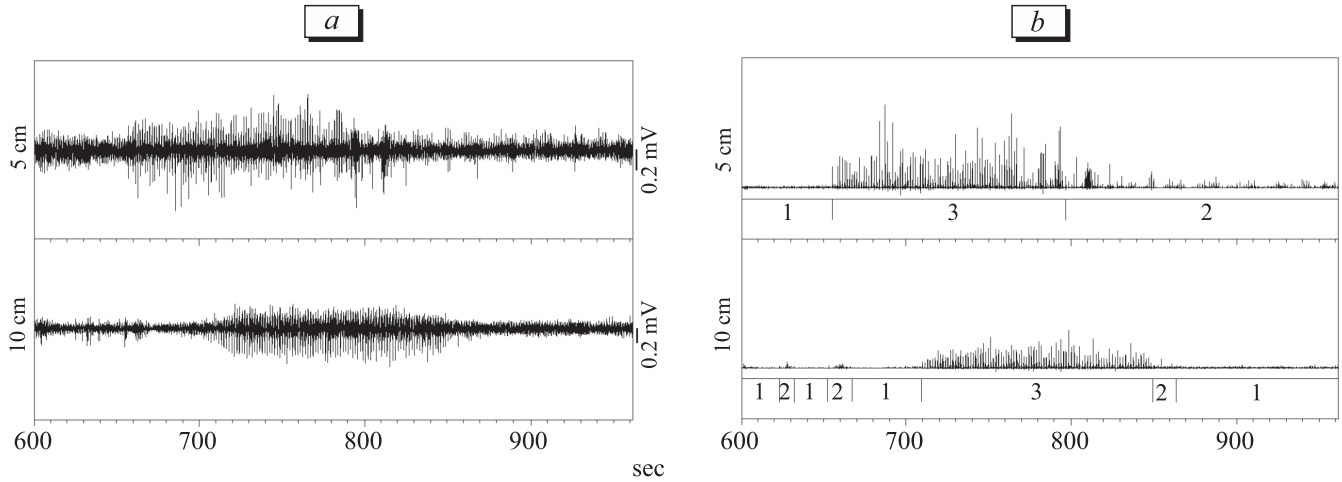

Fig. 3. Spike activity recorded via electrodes positioned at the distances of 5 and 10 cm from the ligament of Treitz. *a*) Initial EMGs; *b*) EMGs processed by a 10-Hz high-pass filter and DEAO. 1) Absence of spike activity; low- (2) and high-amplitude (3) spike activities.

REFERENCES

1. Zherebtsov AV, Tropskaya NS. Application of the Gabor Transform for Analysis of Electromyographic Signals of the Intestine in the Low-Frequency Region. Biophysics. 2018;63(2):248-253.
2. Tropskaya NS, Vasil'ev VA, Popova TS. Minute rhythms of spike activity in intestinal smooth muscles during transition processes. Bull. Exp. Biol. Med. 1996;121(1):32-34.
3. Angeli TR, O'Grady G, Paskaranandavadivel N, Erickson JC, Du P, Pullan AJ, Bissett IP, Cheng LK. Experimental and automated analysis techniques for high-resolution electrical mapping of small intestine slow wave activity. J. Neurogastroenterol. Motil. 2013;19(2):179-191.
4. Beyramienanlou H, Lotfivand N. An efficient teager energy operator-based automated QRS complex detection. J. Healthc. Eng. 2018;2018. ID 8360475. doi: 10.1155/2018/8360475
5. Erickson JC, Velasco-Castedo R, Obioha C, Cheng LK, Angeli TR, O'Grady G. Automated algorithm for GI spike burst detection and demonstration of efficacy in ischemic small intestine. Ann. Biomed. Eng. 2013;41(10):2215-2228.
6. Malik MH, Saeed M, Kamboh AM. Automatic threshold optimization in nonlinear energy operator based spike detection. Conf. Proc. IEEE Eng. Med. Biol. Soc. 2016;2016:774-777.
7. Maragos P, Potamianos A. Higher order differential energy operators. IEEE Signal Proc. Lett. 1995;2(8):152-154.
8. Mukhopadhyay S, Ray G. A new interpretation of nonlinear energy operator and its efficacy in spike detection. IEEE Trans. Biomed. Eng. 1998;45(2):180-187.
9. Renard Y, Lotte F, Gibert G, Congedo M, Maby E, Delannoy V, Bertrand O, Lécuyer A. OpenViBE: an open-source software platform to design, test and use brain-computer interfaces in real and virtual environments. Presence: teleoperators and virtual environments. 2010;19(1):35-53.
10. Sanders KM. Regulation of smooth muscle excitation and contraction. Neurogastroenterol. Motil. 2008;20(Suppl. 1):39-53.
11. Tariq T, Satti MH, Saeed M, Kamboh AM. Low SNR neural spike detection using scaled energy operators for implantable brain circuits. Conf. Proc. IEEE Eng. Med. Biol. Soc. 2017;2017:1074-1077.
12. Wang Z, Chen JD. Blind separation of slow waves and spikes from gastrointestinal myoelectrical recordings. IEEE Trans. Inf. Technol. Biomed. 2001;5(2):133-137.